SCIENTIFIC PROBLEMS
OF MACHINES OPERATION
AND MAINTENANCE
1 (153) 2008

K.CH. WIERZCHOLSKI[*], Y. NYASHIN[**], V. LOGHOV[**]

Contribution in biobearing lubrication

Key words

Biotribology, conjugated fields, numerical calculations.

Słowa kluczowe

Biotribologia, pola sprzężone,obliczenia numeryczne.

Summary

This paper presents the general description of a lubrication problem for two co-operating living cartilage surfaces separated with a bio-fluid in human joints for unsteady boundary conditions. The synovial bio-fluid has visco-elastic properties. The growth of the tissue is taking into account. The congenial growth strain rates in the synovial fluid and in the cartilage are presented in the described bio-tribological model. The tissue occurring in the thin boundary cartilage layer has elastic, hype-elastic, or hypo-elastic properties. Some particular remarks about isotropic growth strains are presented in this paper. Moreover, some cases of pressure distributions and capacities occurring in a human hip joint are obtained in a numerical way.

1. Preliminaries

The biobearing is a living system consisting of solids whose mutual interaction (mechanical, electromagnetic, etc.) is accomplished by bio-fluids.

[*] Gdańsk University of Technology, Narutowicza 11, PL80-952, Gdańsk, Poland.
[**] Perm State Technical University, Russia, Perm, Korolev Street, 614013, Russia: e-mail: nyashin@theormech.pstu.ac.ru

This concept was first introduced by K. Wierzcholski [9] for the description of the behaviour of synovial joints (hip joint, knee joint, ankle joint, etc.). Now, this definition will be extended to other human body elements: tooth with the periodontal ligament, the intervertebral disk, the disks of the temporomandibular joints, etc. It is important to note that this mathematical model can be used for analysis of bioreactors where living tissue is grown. The general scheme of biobearing is shown in Fig. 1.

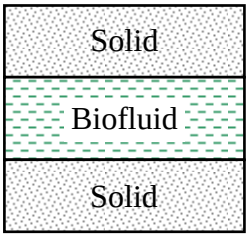

Fig. 1. General scheme of biobearing
Rys. 1. Ogólny schemat biołożyska

Till know, the most detailed results were obtained for natural synovial joints both sound and of different pathologies, as well as for artificial synovial joints. Hence, such natural biobearings will be considered further.

The synovial joint has two main components: a solid one, represented by the cartilage, and biofluid, represented by the synovial fluid. The cartilage is a soft anisotropic solid containing pores filled with a fluid. In the general case, the cartilage can be subjected to large deformations. The synovial fluid contains different molecules: large protein molecules and small molecules of various substances dissolved in water (salts, lipids, etc.).

For a biomechanical description of the cartilage, different models can be used: different models of poromechanics where the solid skeleton is elastic, hyper-elastic, or viscoelastic, either with an ideal fluid or viscous fluid (Biot's model [1]), contained in pores, a model of biphasic solid (Mow's model [5]), and a model of hypo-elastic body (in which viscous properties of liquid in the pores are taken into consideration) [2].

For the biomechanical description of the synovial fluid, different models can be also applied: the model of non-Newtonian liquid [8] or the model of biphasic fluid (consisting of large protein molecules and a water solution of small molecules) [3].

The law of interaction between the cartilage and the synovial fluid is of importance, since the presence of pores makes possible the penetrating of small molecules, but not of large protein molecules.

This structure of synovial joint provides combination of two main functions:

- Low friction (hence low wear), and
- Considerable load capacity maintained for a long period of human life.

Below, we will formulate a mathematical models of the cartilage and synovial fluid, as well as boundary conditions describing mechanical interaction between them.

The living system has some discrepancies as compared with the non-living one, as follows:

– More complicated geometrical forms;
– New constitutive relations;
– Force factors (forces and moments) within human body have been so far investigated insufficiently;
– The problems of mathematical modelling have an interdisciplinary character (as biomechanics, biophysics, biochemistry, anatomy, physiology, etc. are usually involved);
– In living tissues there is a growth strain defined by genetic code and dependent on many other factors (such as temperature, force factors, chemical substances, etc.); and,
– Living organisms must adapt themselves to changing conditions (C. Darwin, Wolff's law).

2. Synovial fluid flow in biobearing gap

The basic equations of living, growing and non-Newtonian biological fluid in the human joint gap are presented in this section. The scheme of the gap is shown in Fig. 2.

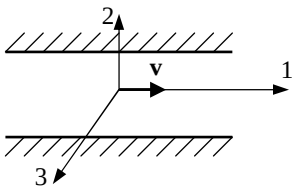

Fig. 2. Scheme of flow region
Rys. 2. Schemat obszaru przepływu

① The equation of motion (or equilibrium) of the biological fluid has the following form:

$$\mathrm{Div}\,\mathbf{S} + \mathbf{F}_b = \rho \frac{d\mathbf{v}}{dt} \tag{2.1}$$

$$\mathbf{S} = \left\| \tau_{ij} \right\| \tag{2.2}$$

where: i, j=1, 2, 3; t is time, **v** is the vector of synovial fluid velocity, **S** is the tensor of synovial fluid stress, τ_{ij} are the components of the stress tensor for i, j=1, 2, 3, and $\mathbf{F}_b$ is the vector of body forces in synovial fluid, ρ is the synovial fluid density.

② The constitutive relation is as follows:

$$\mathbf{S} = \mathbf{S}\left(\mathbf{T}_d, \eta_p, p, T\right) \tag{2.3}$$

where η_p is the apparent viscosity of the synovial fluid, p is hydrodynamic pressure, T is temperature. The total strain rate tensor $\mathbf{T}_d$ in the synovial fluid has the following form:

$$\mathbf{T}_d = \mathbf{T}_d^h + \mathbf{T}_d^g \text{ or } \mathbf{T}_d = \left\| \Theta_{ij} \right\| = \left\| \Theta_{ij}^h \right\| + \left\| \Theta_{ij}^g \right\| \tag{2.4}$$

$$\mathbf{T}_d^g = \mathbf{C}^c + \mathbf{C}^g : \mathbf{S} \tag{2.5}$$

$$\mathbf{T}_d^h = \left\| \Theta_{ij}^h \right\| \tag{2.6a}$$

$$\mathbf{C}^c = \left\| C_{ij}^c \right\| \tag{2.6b}$$

$$\mathbf{C}^g = \left\| C_{ijkn}^g \right\| \tag{2.6c}$$

The formula (2.6a) describes the hydrodynamic strain rate tensor in the synovial fluid with the components Θ_{ij}^h for i, j=1, 2, 3. We denote: $\mathbf{C}^c$ is the congenial growth strain rate tensor of the synovial fluid, see Equation (2.6b) and C_{ij}^c are the components of congenial growth strain rate tensor in the synovial fluid. Symbol Θ_{ij} in Equation (2.4) describes the components if the total strain rate tensor in the fluid. Additionally, we denote: Θ_{ij}^g are the components of the growth strain rate tensor in fluid, C_{ijkn}^g are the components of the $\mathbf{C}^g$ tensor, $\mathbf{T}_d^g$ and is the growth strain rate tensor.

③ The geometrical relations are presented below:

$$\mathbf{T}_d = \frac{1}{2}\left(\text{grad } \mathbf{v} + (\text{grad } \mathbf{v})^T\right) \equiv \frac{1}{2}\mathbf{A}_1 \tag{2.7}$$

④ The equation of continuity of the growing fluid has the following form:

$$\frac{\partial \rho}{\partial t} + \text{div}(\rho \mathbf{v}) = M_q \tag{2.8}$$

where M_q is the mass source per unit of time and volume.

3. Rheological properties of synovial liquids

It is possible to select a wide class of fluids that have the property of remembering their deformation history and exhibiting the elastic properties [6].

The dominant part of rheological equations is formulated in terms of the excessive-stress or extra-stress tensor $\mathbf{S}_{ex,}$ which is not a deviator tensor. In this case, the total stress tensor **S** is decomposed into two summands:

$$\mathbf{S} = -p_{hs}\mathbf{I} + \mathbf{S}_{ex}\,,\ p = -\frac{1}{3}\text{tr}(\mathbf{S}) = p_{hs} - \frac{1}{3}\text{tr}(\mathbf{S}_{ex}) \tag{3.1}$$

where p_{hs} is the hydrostatic pressure, $\mathbf{S}_{ex}$ is the excessive stress tensor determined by rheological equation. To construct rheological equations for viscoelastic fluids, it is necessary to solve the problem of defining the elasticity of the fluid. In the theory of elasticity, it is assumed that internal stresses are defined by deformations with respect to a reference configuration, the preferable configuration of material. On the contrary, liquid materials are those of no preferable configuration.

This contradiction is resolved by determining deformation, not with respect to preferable configuration but by the distinction between an actual configuration and the preceding one.

In other words, elastic solids have a permanent memory of preferable configuration. Ideally, viscous fluids have no memory and are sensitive to an instantaneous strain rate.

A general theory of materials with memory is the theory of simple fluid developed by Noll and Koleman. The simple fluid theory is based on the assumption that stress is defined by a whole deformation history and the following four concepts:

1) ***determinism*** – stresses are defined by the previous deformation history and do not depend on future deformations;
2) ***local action*** – stresses in a point are uniquely determined by the deformation history of the small neighbourhood of the point;
3) ***non-existence of natural non-stressed state*** – fluid has not a preferable form and all possible forms are equivalent; and,
4) ***fading memory*** – influence of deformation is smaller at distant points of time than near ones.

In the case of slow flows, the principle of fading memory renders the m-order approximation of the general rheological equation in the form:

$$\mathbf{S}_{ex} = \mathbf{M}\left(\mathbf{A_1}, \mathbf{A_2}, \ldots, \mathbf{A}_m\right) \tag{3.2}$$

where **M** is an isotropic function.

Rivlin–Ericksen tensors are defined by the recurrent formula:

$$\mathbf{A}_{m+1} = \frac{d}{dt}\mathbf{A}_m + \mathbf{L}^T\mathbf{A}_m + \mathbf{A}_m\mathbf{L} \tag{3.3a}$$

$$\mathbf{A}_0 \equiv \mathbf{I}, \quad \mathbf{A}_1 \equiv \mathbf{L} + \mathbf{L}^T, \quad \mathbf{A}_2 \equiv \operatorname{grad}\mathbf{a} + (\operatorname{grad}\mathbf{a})^T + 2\mathbf{L}^T\mathbf{L}, \ldots \tag{3.3b}$$

$$\mathbf{a} \equiv \frac{\partial \mathbf{v}}{\partial t} + \mathbf{L}\mathbf{v}, \quad \mathbf{L} \equiv (\operatorname{grad}\mathbf{v})^T, \quad \mathbf{L}^T \equiv \operatorname{grad}\mathbf{v} \tag{3.3c}$$

where m=1, 2, 3,…. We denote: **a** is the acceleration vector, **L** is the transpose tensor of gradient of fluid velocity vector. The notion **Lv** stands for the tensor inner product of the tensors **L** and **v**. Application of the Hamilton–Cayley [7] theorem to the Equation (3.2) yields the excessive stress tensor in the following form:

$$\mathbf{S}_{ex} = \eta(\Theta, p, T)\mathbf{A}_1 + \alpha(\Theta)\mathbf{A}_1\mathbf{A}_1 + \beta(\Theta)\mathbf{A}_2 \tag{3.4}$$

where η, α, β are the liquid dynamic viscosity and pseudo-viscosities, respectively, Θ is the scalar characteristic of strain rate tensor.

4. Growing cartilage deformations

The statement of the initial boundary value problem for the growing cartilage is as follows:

① The equation of motion (or equilibrium) for cartilage has the following form:

$$\mathrm{Div}\,\mathbf{S}^{*}+\mathbf{F}_{b}^{*}=\rho^{*}\frac{d\mathbf{v}^{*}}{dt} \tag{4.1}$$

$$\mathbf{S}^{*}=\left\|\tau_{ij}^{*}\right\| \tag{4.2}$$

where i, j=1, 2, 3; t is time, $\mathbf{v}^{*}$ is the velocity vector of the cartilage particle, $\mathbf{S}^{*}$ is the stress tensor in the cartilage layer, τ_{ij}^{*} are the components of the stress tensor in the cartilage, $\mathbf{F}_{b}^{*}$ is the vector of body forces in the cartilage, ρ^{*} is the cartilage density. Here, we neglect the terms related to mass sources.

② The constitutive relation for bone or cartilage is as follows:

$$\mathbf{T}_{d}^{*}=\mathbf{T}_{d}^{e*}+\mathbf{T}_{d}^{g*},\ \text{or}\ \mathbf{T}_{d}^{*}=\left\|\Theta_{ij}^{*}\right\|=\left\|\Theta_{ij}^{e*}\right\|+\left\|\Theta_{ij}^{g*}\right\| \tag{4.3}$$

$$\mathbf{T}_{d}^{g*}=\mathbf{C}^{c*}+\mathbf{C}^{g*}:\mathbf{S}^{*} \tag{4.4a}$$

$$\mathbf{C}^{c*}=\left\|C_{ij}^{c*}\right\| \tag{4.4b}$$

$$\mathbf{C}^{g*}=\left\|C_{ijkn}^{g*}\right\| \tag{4.4c}$$

for i, j, k, n=1, 2, 3. We use the following notations: Θ_{ij}^{*} are the components of the total strain rate tensor in the cartilage, Θ_{ij}^{e*} are the components of elastic strain rate tensor in the cartilage, Θ_{ij}^{g*} are the components of growth strain rate tensor in the cartilage, $\mathbf{C}^{c*}$ is the congenial growth tensor of the cartilage, C_{ij}^{c*} are the components of congenial growth tensor in cartilage, $\mathbf{C}^{g*}$ is the tensor of stress influence on the cartilage growth, C_{ijkn}^{g*} are the components of the $\mathbf{C}^{g*}$ tensor, $\mathbf{T}_{d}^{e*}$ is the elastic strain rate tensor (in particular, including hyperelastic, hypoelastic, and viscoelastic constituents), $\mathbf{T}_{d}^{g*}$ is growth strain rate tensor.

Further, we specify the constitutive relation for porous cartilage. The porous cartilage can be considered as hypoelastic. The theory of hypoelasticity

was formulated by Truesdell. Noll showed later that hypoelasticity is the most general form of elasticity. In a hypoelastic model, an objective stress rate $\mathbf{S}^{\nabla *}$ is dependent on the rate of deformation $\mathbf{T}_{\mathrm{d}}^{\mathrm{e}*}$ according to the following equation:

$$\mathbf{S}^{\nabla *} = \mathbf{C}^{\mathrm{hy}*} : \mathbf{T}_{\mathrm{d}}^{\mathrm{e}*} \quad \text{or} \quad \mathbf{T}_{\mathrm{d}}^{\mathrm{e}*} = (\mathbf{C}^{\mathrm{hy}*})^{-1} : \mathbf{S}^{\nabla *} \tag{4.5}$$

$$\mathbf{C}^{\mathrm{hy}*} = \left\| C_{\mathrm{ijkn}}^{\mathrm{hy}*} \right\| \tag{4.6}$$

where: i, j, k, n=1, 2, 3. $\mathbf{C}^{\mathrm{hy}*}$ is the hypo-elasticity tensor of the fourth rank with the components $C_{\mathrm{ijkn}}^{\mathrm{hy}*}$, $\mathbf{S}^{\nabla *}$ is the objective stress rate tensor. The objective stress rate is invariant to rigid body rotation. Many expressions for objective stress rates have been proposed, including those proposed by Truesdell, Jaumann–Noll, etc.

The necessity of objective stress rate is associated with the fact that time derivatives calculated in the reference frame moving together with the representative material element and those calculated in the immovable reference frame are different. Hence, when calculating the time derivative in the immovable reference frame, it is necessary to consider the movement of the moving reference frame, and for tensor $\mathbf{S}^{*}$, to use the co-rotational (objective) derivative by Jaumann-Noll (or other co-rotational ones):

$$\mathbf{S}^{\nabla *} \equiv \dot{\mathbf{S}}^{*} - \boldsymbol{\Omega}_{\mathrm{v}}^{*}\mathbf{S}^{*} + \mathbf{S}^{*}\boldsymbol{\Omega}_{\mathrm{v}}^{*}, \qquad (\dot{\ }) \equiv \frac{\mathrm{d}}{\mathrm{dt}}(\ \ ) \tag{4.7}$$

where

$$\boldsymbol{\Omega}_{\mathrm{v}}^{*} \equiv \frac{1}{2}\left[\left(\mathrm{grad}\mathbf{v}^{*}\right)^{\mathrm{T}} - \mathrm{grad}\mathbf{v}^{*} \right] \tag{4.8}$$

is the vorticity tensor.

The physical meaning of Jaumann–Noll derivative lies in the fact that it allows us to determine a tensor change relative to the moving reference frame. During the change, this system is moving together with a representative continuum volume having the angular velocity $\boldsymbol{\omega} \equiv 0.5\ \mathrm{rot}\ \mathbf{v}$.

② The geometrical relations for bone and cartilage are defined in the following form:

$$\mathbf{T}_{\mathrm{d}}^{*} = \frac{1}{2}\left(\mathrm{grad}\ \mathbf{v}^{*} + (\mathrm{grad}\ \mathbf{v}^{*})^{\mathrm{T}}\right) \tag{4.9}$$

$$\mathbf{v}^* = \frac{d\mathbf{u}^*}{dt}, \quad \mathbf{u}^* = \int_0^t \mathbf{v}^* \, dt + \mathbf{u}_0^* \tag{4.10}$$

where $\mathbf{u}_0^*$ is the initial displacement vector.

The constitutive relations in which growth strain is taken into consideration have been proposed by Feng-Hsiang Hsu [4].

5. Some remarks about isotropic growth strain

Here, we discuss in detail the important property of living tissues − their capability of growing. To this end, we introduce the following definitions:

* The growth is the process of the change of the mass of a biological system defined by genetic (congenital) factors and dependent on epigenetic (environmental) factors (temperature, mechanical stress and strain, chemical substances, internal and external physical fields, *etc*.).
* The remodelling (or adaptation) is the process of the change of shape and the properties of a biological system defined by change of internal and/or external conditions.
* The external remodelling is the process of change of shape of the system.
* The internal remodelling is the process of the change of properties of the system (mechanical properties of trabeculae, their architecture, development of pores, etc.).

Sometimes the process of the change of the shape of the system is called the morphogenesis. In the general sense, the tensors $\mathbf{C}^{c*}$ and $\mathbf{C}^{g*}$ depend on time and coordinates of position.

Let us assume that growth strains are isotropic in the domain under consideration, i.e. the components of the tensors $\mathbf{C}^{c*}$ and $\mathbf{C}^{g}$ do not depend on a turning (and reflection) of the Cartesian orthogonal coordinates system. In this case, we have the so-called isotropic tensors whose components do not depend on a turning (and reflection) of coordinate axes. Hence, it follows that these components do not depend on the orthogonal transformation of basis vectors.

As known, among the second rank tensors there is only one linearly independent isotropic tensor as follows:

$$C_{ij}^{c*} = C^{c*} \, \delta_{ij} \tag{5.1}$$

where δ_{ij} is Kronecker symbol and i, j=1, 2, 3.

Among the fourth rank tensors, there are three linearly independent tensors, which can be used as $\mathbf{C}^{g*} \equiv \left\| C^{g*}_{ijkn} \right\|$ tensors as follows:

$$\delta_{ij}\delta_{kn}, \quad \delta_{ik}\delta_{jn} \pm \delta_{in}\delta_{jk} \tag{5.2}$$

In the general case, we represent the components of $\mathbf{C}^{g*}$ tensor as a linear combination as follows:

$$C^{g*}_{ijkn} = \pi_1\delta_{ij}\delta_{kn} + \pi_2(\delta_{ik}\delta_{jn} + \delta_{in}\delta_{jk}) + \pi_3(\delta_{ik}\delta_{jn} - \delta_{in}\delta_{jk}) \tag{5.3}$$

where i, j, k, n=1, 2, 3; π_1, π_2, π_3 denote empirical constants in $(\text{Pas})^{-1}$.

It is easy to calculate

$$(\mathbf{C}^{g*}:\mathbf{S}^{*})_{ij} = C^{g*}_{ijkn}\tau^{*}_{kn} = \pi_1\delta_{ij}\tau^{*}_{kk} + \pi_2(\tau^{*}_{ij} + \tau^{*}_{ji}) + \pi_3(\tau^{*}_{ij} - \tau^{*}_{ji}) \tag{5.4}$$

$$C^{g*}_{ijkn}\tau^{*}_{kn} = \pi_1\delta_{ij}\tau^{*}_{kk} + 2\pi_2\tau^{*}_{ij} \tag{5.5}$$

where the symmetry of stress tensor is assumed and

$$\tau^{*}_{kk} = \tau^{*}_{11} + \tau^{*}_{22} + \tau^{*}_{33} \equiv I_1(\mathbf{S}^{*}) \tag{5.6}$$

is the first invariant of the stress tensor $\mathbf{S}^{*}$.

Finally, the growth strain rate has the following form:

$$\Theta^{g*}_{ij} = C^{c*}\,\delta_{ij} + \pi_1\delta_{ij}\tau^{*}_{kk} + 2\pi_2\tau^{*}_{ij} \tag{5.7}$$

In many cases, it is convenient to decompose stress tensor into spherical tensor and deviator tensor.

$$\tau^{*}_{ij} = \frac{1}{3}\tau^{*}_{kk}\delta_{ij} + \tau^{d*}_{ij} \tag{5.8}$$

$$\mathbf{S}^{*} = \mathbf{S}^{o*} + \mathbf{S}^{d*} \tag{5.9}$$

Symbol $\mathbf{S}^{d*}$ denotes the deviator stress tensor in cartilage. We put (5.8) into (5.7) and obtain the following:

$$\Theta_{ij}^{g*} = C^{c*}\delta_{ij} + \frac{1}{\pi_4}\delta_{ij}\tau_{kk}^{*} + \frac{1}{2\pi_5}\tau_{ij}^{d*} \tag{5.10}$$

with

$$2\pi_2 \equiv \frac{1}{2\pi_5}, \quad \pi_1 + \frac{2\pi_2}{3} \equiv \frac{1}{\pi_4} \tag{5.11}$$

If we consider the elastic material (in the case of small deformations), then we can take into account the well-known Hooke's relation:

$$\varepsilon_{ij}^{e} = \frac{1}{3K}\delta_{ij}\tau_{kk} + \frac{1}{2G}\tau_{ij}^{d} \tag{5.12}$$

with the elastic moduli

$$G = \frac{E}{2(1+\nu)}, \quad K = \frac{E}{1-2\nu}, \quad \tau_{kk} = K\varepsilon_{kk} \tag{5.13}$$

We denote: K is the bulk modulus, G is the shear modulus, E is the elasticity modulus of cartilage, and ν is Poisson's ratio. Differentiation of both sides of Equation (5.12) with respect to time t (the dot above is the symbol of time differentiation) gives the following:

$$\Theta_{ij}^{e} = \frac{d\varepsilon_{ij}^{e}}{dt} = \frac{1}{3K}\delta_{ij}\dot{\tau}_{kk}^{*} + \frac{1}{2G}\dot{\tau}_{ij}^{d*}. \tag{5.14}$$

It is evident that Equations (5.10) and (5.14) are almost similar to each other. Apart from the term containing $\mathbf{C}^{c*}$ tensor and the change of stress rate to stress, the following difference between (5.10) and (5.14) can be observed: from the second law of thermodynamics it follows that in (5.14) $G \geq 0$, $K \geq 0$ and as a result

$$-1 \leq \nu \leq 1/2. \tag{5.15}$$

The inequality (5.15) is not valid for the growth of strains presented in relation (5.10). Therefore, the relation (5.10) can be written in the tensor form as follows:

$$\mathbf{T}_{d}^{g*} = \left\| \Theta_{ij}^{g*} \right\| = \left(C^{c*} + \frac{I_1(\mathbf{S}^{*})}{\pi_4} \right)\mathbf{I} + \frac{1}{2\pi_5}\mathbf{S}^{d*} \tag{5.16}$$

$$\mathbf{I} = \left\| \delta_{ij} \right\| \tag{5.17}$$

The symbol **I** stands for unit tensor. To make the next simplifications, we take the following assumptions for Equation (5.7):

$$\pi_1 = 0, \quad \pi_2 \equiv C^{g*} \tag{5.18}$$

By virtue of the assumption (5.18), equation (5.5) yields

$$(\mathbf{C}^{g*} : \mathbf{S}^*)_{ij} = C^{g*} \tau_{ij}^* \tag{5.19}$$

Equation (5.7) can be reduced to the following form:

$$\Theta_{ij}^{g*} = C^{c*} \delta_{ij} + C^{g*} \tau_{ij}^* \tag{5.20}$$

The formula (5.20) has the following tensorial form:

$$\mathbf{T}_d^{e*} = C^{c*} \mathbf{I} + C^{g*} \mathbf{S}^* \tag{5.21}$$

For uniaxial case, we have

$$\Theta^{g*} = C^{c*} + C^{g*} \tau^* \tag{5.22}$$

Every human joint undergoes stages of evolution and involution (back process). In the stage of evolution: $C^{c*} > 0$, and in the stage of involution: $C^{c*} < 0$.

Let us suppose that in relation (5.21) $C^{g*} > 0$. In this case, tension will stimulate growth and compression will suppress growth (Hüter–Volkman's law, 18th century).

It can be observed that, if we put $C^{c*} = 0$ into the relation (5.21), then it coincides with that for viscous fluid.

6. Initial and boundary conditions

Let us consider the domain V with boundary S presented in Fig. 3. The closure $\overline{V}$ belongs to three-dimensional Euclidean space E^3. Let us suppose that the boundary surface of the cartilage−bio-fluid system is divided into three disjoint parts:

$$S = S_v \cup S_\sigma \cup S_c \tag{6.1}$$

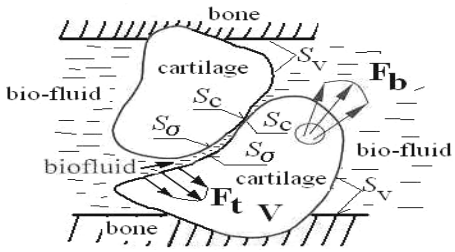

Fig. 3. The region formed by two cartilages and bio-fluid
Rys. 3. Obszar utworzony przez dwie chrząstki i ciecz biologiczną

At the boundary S_v, between the cartilage or bone surface and the synovial fluid, the kinematical boundary condition is given as follows:

$$\mathbf{v} = \bar{\mathbf{v}}, \quad \mathbf{r} \in S_v \tag{6.2}$$

where $\bar{\mathbf{v}}$ is the given velocity at boundary S_v and $\mathbf{r}$ is the position vector. At every point, three components of the velocity vector are given.

At the surface S_σ, between the superficial layer of the cartilage and the thin layer of the synovial fluid, the dynamical boundary condition is assumed as follows:

$$\mathbf{nS}=\mathbf{F}_t, \mathbf{r} \in S_\sigma \tag{6.3}$$

where $\mathbf{n}$ is unit outside normal vector, $\mathbf{F}_t$ is the given vector of the surface traction. At every point, the components of stress tensor are given.

At the contact surface S_c, between the boundary thin layers of the fluid and the cartilage, we suppose the adhesion condition:

$$\mathbf{v} = \mathbf{v}^*, \mathbf{r} \in S_c \tag{6.4}$$

where $\mathbf{v}^*$ is the velocity of cartilage particle and $\mathbf{v}$ is the velocity of contacting fluid particle. The form of the contact boundary is determined by cartilage layer deformation.

The initial conditions are as follows:

$$\rho, \mathbf{v}, \mathbf{S} \text{ are given for } t = 0 \tag{6.5}$$

at every point of biobearing.

7. Numerical examples for squeezing lubrication of human hip joint

Now, we show numerical calculations of pressure distribution during the squeezing lubrication in human hip joint. Two curvilinear bone surfaces separated with the joint gap of small height come up with uniform motion of velocity U. This velocity is caused by the human limbs' motion. A small region of the least gap height between surfaces (or of contact of surfaces) is assumed to be a circle or ellipse, approximately. This region of bone surface can be recognised as plane surface by virtue of its very small size as compared with diameter of bone head. Let us consider the spherical coordinates. Dependencies between the rectangular (x,y,z) and spherical ($\alpha_1=\varphi,\alpha_2=r$, $\alpha_3=\vartheta$) co-ordinates have the following form:

$$x = r\sin(\vartheta/R)\cos\varphi,\quad y=r\sin(\vartheta/R)\sin\varphi,\ z = r\cos(\vartheta/R),\ 0<r<R \tag{7.1}$$

Graphical illustration of the centre of spherical bone head O(0,0,0), and the centre of spherical acetabulum in point $O_1(x-\Delta\varepsilon_x, y-\Delta\varepsilon_y, z+\Delta\varepsilon_z)$ in human hip joint is presented in Fig. 4. The equation of spherical acetabulum surface can be written in the following form:

$$(x-\Delta\varepsilon_x)^2+(y-\Delta\varepsilon_y)^2+(z+\Delta\varepsilon_z)^2=(R+D+\varepsilon_{min})^2,\ D=[(\Delta\varepsilon_x)^2+(\Delta\varepsilon_y)^2+(\Delta\varepsilon_z)^2]^{0.5} \tag{7.2}$$

We put the dependencies (7.1) in Equation (7.2), hence we obtain:

$$(r\cos\varphi\sin\alpha_3/R-\Delta\varepsilon_x)^2+(r\sin\varphi\sin\alpha_3/R-\Delta\varepsilon_y)^2+(r\cos\alpha_3/R+\Delta\varepsilon_z)^2 = \\ = (R+D+\varepsilon_{min})^2 \tag{7.3}$$

The gap height has the following form:

$$\varepsilon(\varphi,\alpha_3/R)\equiv r-R \tag{7.4}$$

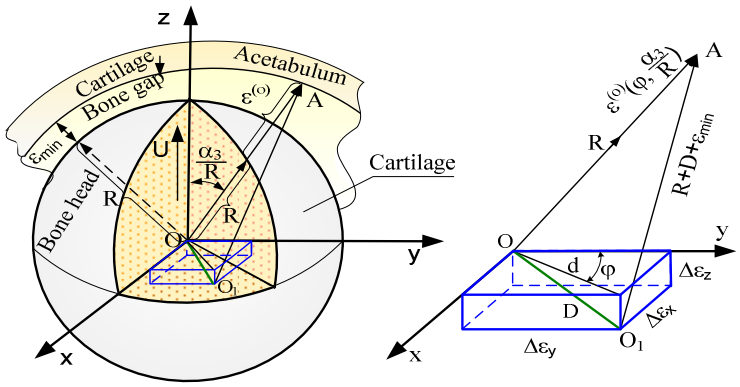

Fig. 4. Centre O_1 of spherical acetabulum surface and centre O of spherical bone head
Rys. 4. Środek O_1 sferycznej powierzchni panewki oraz środek O sferycznej głowy kostnej

We find the unknown r from Equation (7.3) and put it into the formula (7.4). Hence the gap height finally has the following form:

$$\varepsilon(\varphi,\alpha_3/R)=\Delta\varepsilon_x\cos\varphi\,\sin\alpha_3/R+\Delta\varepsilon_y\,\sin\varphi\,\sin\alpha_3/R-\Delta\varepsilon_z\,\cos\alpha_3/R-R+$$
$$+[(\Delta\varepsilon_x\cos\varphi\,\sin\alpha_3/R+\Delta\varepsilon_y\,\sin\varphi\,\sin\alpha_3/R-\Delta\varepsilon_z\,\cos\alpha_3/R)^2+$$
$$+(R+\varepsilon_{min})(R+2D+\varepsilon_{min})]^{0.5} \qquad (7.5)$$

We assume the following: $\Delta\varepsilon_x=-5$ μm, $\Delta\varepsilon_y=-5$ μm, $\Delta\varepsilon_z=+5$ μm, $\theta_3=1/10$, the radius of bone head R=0.026575 m and atmospheric pressure on the round of the region $\Omega(\alpha_1,\alpha_3)$: $\{0<\alpha_1\equiv\varphi\le 2\pi,\ 0<\alpha_3\equiv\vartheta\le R\pi/10\}$ resting on bone head (see Fig. 5). The lubrication surface area has value of $2\pi R^2[1-\cos(\pi/10)]\approx 2.17$ cm^2.

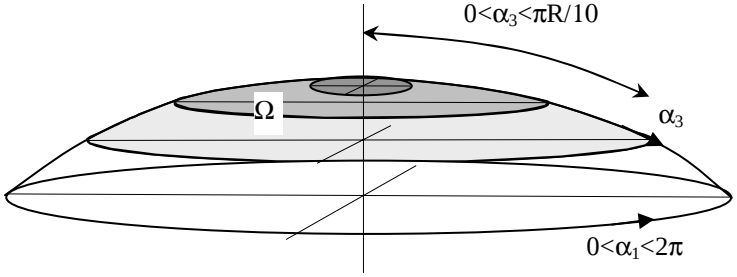

Fig. 5. Region of pressure distribution resting on bone head
Rys. 5. Obszar rozkładu ciśnienia spoczywający na głowie kostnej

In calculations, for a normal hip joint, we took the smallest gap height $\varepsilon_{min}=60$ μm i.e. $D+\varepsilon_{min}=67$ μm. Taking into account the uniform velocity of bone head U=0.01 m/s and the average value of synovial fluid dynamic viscosity $\eta_o=2.00$ Pas or $\eta_o=1.00$ Pas, for $0<\alpha_1\equiv\varphi\le 2\pi$, $0<\alpha_3\equiv\vartheta\le R\pi\theta_3$, $0<\alpha_2\equiv r\le\varepsilon$, where $\theta_3\in[0,1/10]$, we solve the following Reynolds equation:

$$\frac{1}{R\sin\frac{\vartheta}{R}}\frac{\partial}{\partial\varphi}\left(\frac{\varepsilon^3}{\eta}\frac{\partial p}{\partial\varphi}\right)+\frac{\partial}{\partial\vartheta}\left(R\sin\left(\frac{\vartheta}{R}\right)\frac{\varepsilon^3}{\eta}\frac{\partial p}{\partial\vartheta}\right)=-12\,UR\sin\frac{\vartheta}{R} \qquad (7.6)$$

where the hydrodynamic pressure p has its maximum value equal to 17.13×10^6 Pa$\approx$ 171.3 at or 8.61×10^6 Pa, and the capacity $C_{tot}=2494$ N or $C_{tot}=1247$ N.

Taking into account the uniform velocity of bone head U=0.05 m/s, and the average value of synovial fluid dynamic viscosity $\eta=0.30$ Pas or $\eta=0.10$ Pas, we obtain from Equation (7.6) that the hydrodynamic pressure p has its maximum value equal to 12.87×10^6 Pa$\approx$ 128.7 at or $4{,}36\times10^6$Pa. The capacity in above two cases has values $C_{tot}=1870$ N or 624N (see Fig. 6).

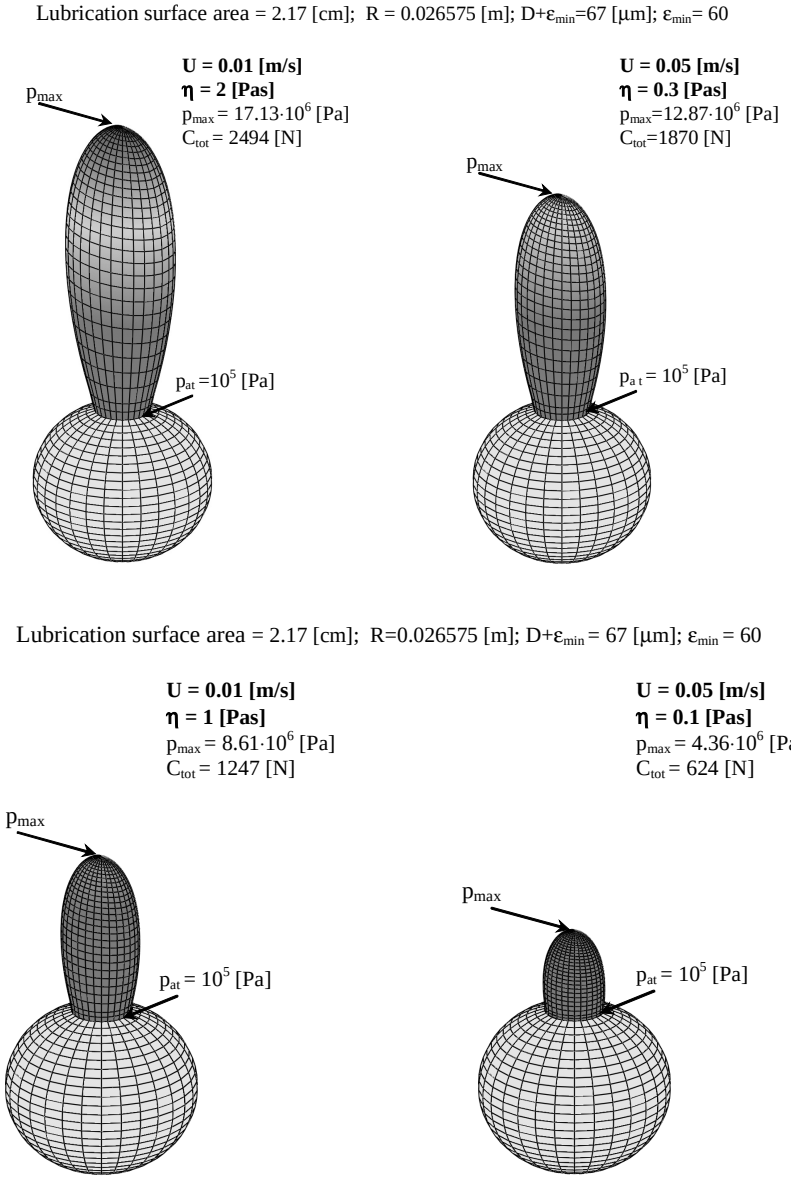

Fig. 6. Four cases of pressure distribution in normal spherical hip joint for squeezing
Rys. 6. Cztery przypadki rozkładu ciśnienia dla zdrowego sferycznego stawu biodrowego przy wyciskaniu

For calculations of a pathological hip joint, we take the smallest gap height ε_{min}=30 μm i.e. D+ε_{min}=37 μm. Taking into account the uniform velocity of bone head, U=0.01 m/s, and the average value of synovial fluid dynamic viscosity η_o=0.1 Pas or η=0.05 Pas, we obtain from Equation (7.6) that the hydrodynamic pressure p has its maximum value equal to 6.30×10^6 Pa≈ 63 at or 3.20×10^6 Pa

and the carrying capacity C_{tot}= 903 N or C_{tot} = 452 N. Taking into account the uniform velocity of bone head U=0.05 s^{-1}, and the average value of synovial fluid dynamic viscosity η=0.03 Pas or η=0.01 Pas, we obtain from Equation (7.6) that the hydrodynamic pressure p has its maximum value equal to 9.42×10^6 Pa≈ 94,2 at or 3.20×10^6 Pa. The contact surface area has the value of ≈2.17 cm^2 and the capacity in above two cases has values C_{tot}=1354 N or 452N (see Fig. 7).

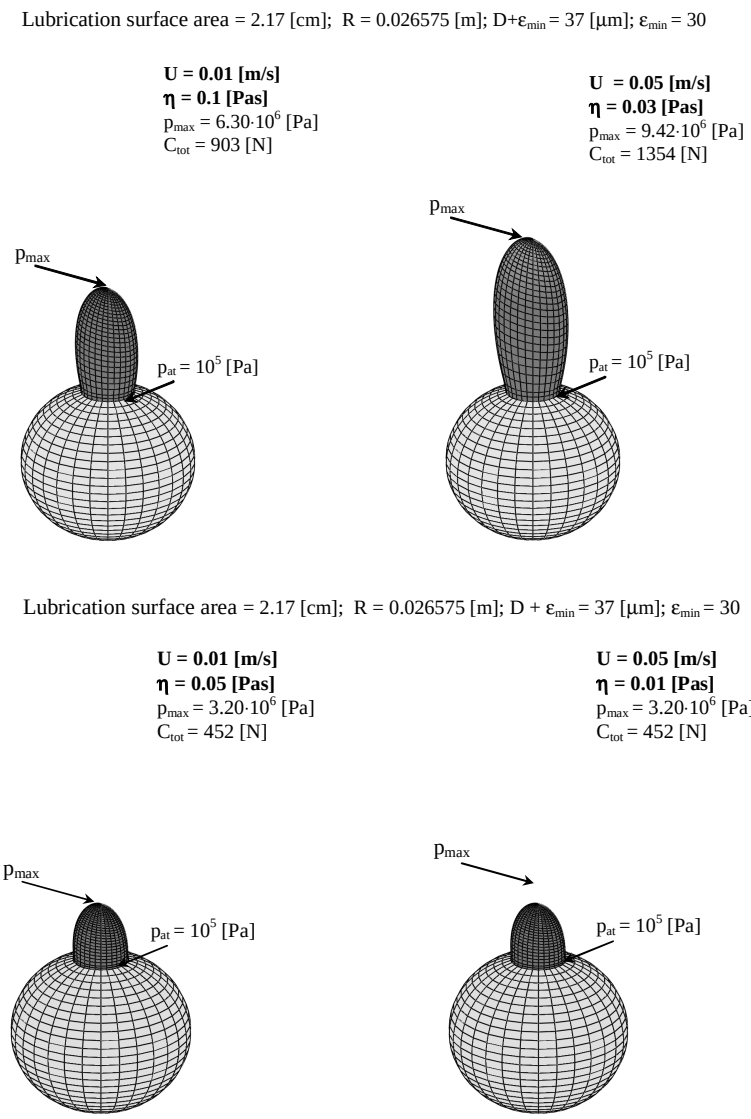

Fig. 7. Four cases of pressure distribution in pathological spherical hip joint for squeezing
Rys.7. Cztery przypadki rozkładu ciśnienia dla chorego sferycznego stawu biodrowego przy wyciskaniu

7.1. Conclusions

The present intersection shows the general analytical description of the considered lubrication squeeze flow problem. Moreover, we have given analytical and numerical methods of solutions, and general analytical solutions of the human joint lubrication problem in spherical co-ordinates for the squeeze fluid lubrication flow that occurs in human joint gap.

In particular cases, all the obtained results tend to simple particular solutions well known in the classical lubrication theory described in spherical co-ordinates. In contrast with the papers of Mow [5], the present section shows a unification and analytical method of solutions of the lubrication problem in human spherical joint gap.

8. Capacity forces in human hip joint for hydrodynamic lubrication by rotation

Now, we can show the numerical calculations of pressure distribution during the hydrodynamic lubrication caused by rotation in the human hip joint. The Reynolds equation for hydrodynamic lubrication caused by the rotation of the spherical bone head follows from Equation (2.1) and has the following form:

$$\frac{\partial}{\partial\varphi}\left(\frac{\varepsilon^3(u_2)}{\eta}\frac{\partial p}{\partial\varphi}\right)+R^2\sin\left(\frac{\vartheta}{R}\right)\frac{\partial}{\partial\vartheta}\left[\frac{\varepsilon^3(u_2)}{\eta}\frac{\partial p}{\partial\vartheta}\sin\left(\frac{\vartheta}{R}\right)\right]= 6\omega R^2\frac{\partial\varepsilon(u_2)}{\partial\varphi}\sin^2\left(\frac{\vartheta}{R}\right) \tag{8.1}$$

where: $0<\alpha_1\equiv\varphi<\pi$, $\pi R/8<\alpha_3\equiv\vartheta<\pi R/2$.

Symbol u_2 obtained from (4.1) denotes cartilage deformation in the radial direction. In the numerical calculations, we assume the following values for joint gap: $\Delta\varepsilon_x$=2 μm, $\Delta\varepsilon_y$=2 μm, $\Delta\varepsilon_z$=+2 μm, radius of bone head R=0.026575 m. In the calculations for a normal hip joint, we assume in calculations the smallest gap height ε_{min}=2.0 μm. Taking into account the angular velocity of the bone head ω=1 s^{-1} and an average value of the dynamic viscosity of synovial fluid η_o=0.03 Pas, we obtain from Equation (8.1) that the hydrodynamic pressure $p^{(o)}$ has its maximum value equal to 1.11×10^6 N/m^2, and the capacity C_{tot}=673 N. Taking into account the angular velocity of the bone head ω = 0.1 s^{-1} and an average value of the dynamic viscosity of synovial fluid η=0.40 Pas, we obtain from Equation (8.1) that the hydrodynamic pressure p has its maximum value equal to 1.44×10^6 N/m^2 and the carrying capacity C_{tot} = 897 N (see Fig. 8. The lubrication surface value is $\pi R^2\cos\pi/8\approx20.38$ cm^2.

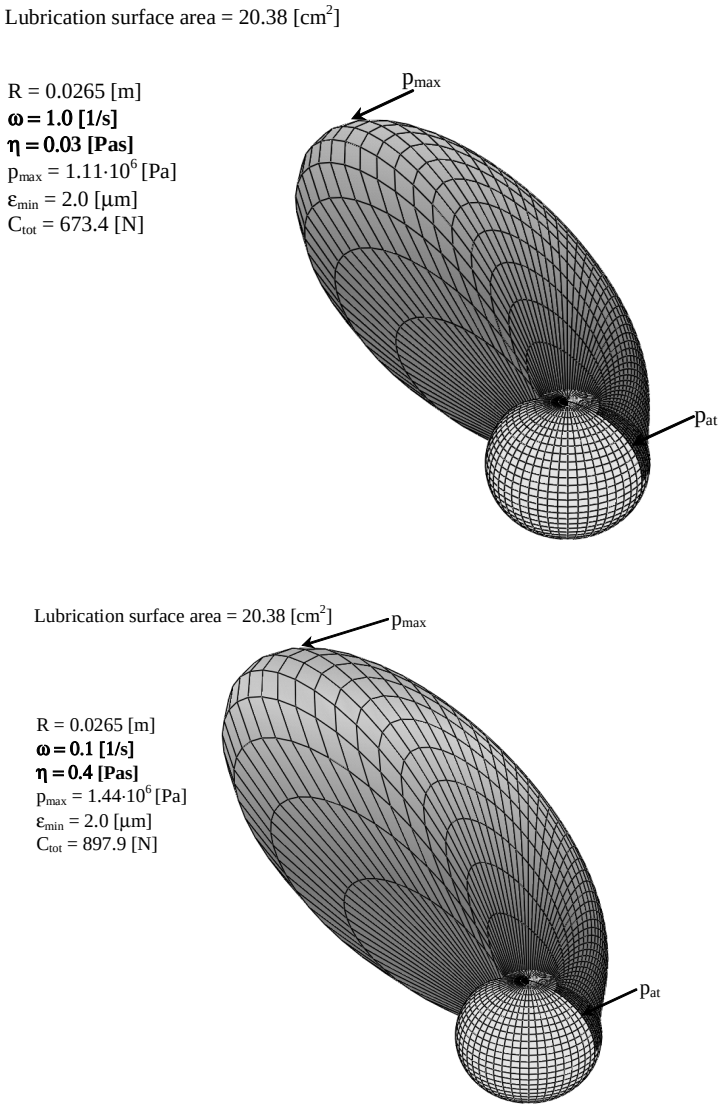

Fig. 8. Two cases of pressure distribution in normal spherical hip joint gap during hydrodynamic lubrication caused by rotation
Fig. 8. Dwa przypadki rozkładu ciśnienia dla zdrowego sferycznego stawu biodrowego podczas hydrodynamicznego smarowania wywołanego ruchem obrotowym

In the calculations for a pathological hip joint, we assume in calculations the smallest gap height ε_{min}=1.0 μm. For the angular velocity of the bone head $\omega = 1\ s^{-1}$ and an average value of dynamic viscosity of synovial fluid $\eta_o = 0.005$ Pas, we obtain from Equation (8.1) that the hydrodynamic pressure p has its maximum value equal to 0.76×10^6 N/m^2 and the carrying capacity C_{tot} = 341 N.

Taking into account the angular velocity of the bone head $\omega=0.1\ s^{-1}$ and an average value of the dynamic viscosity of synovial fluid $\eta=0.07$ Pas, we obtain from Equation (8.1) that the hydrodynamic pressure $p^{(o)}$ has its maximum value equal to 1.034×10^6 N/m^2 and the carrying capacity C_{tot} = 477.5 N. These pressure distributions on the bone head for the gaps of the normal and pathological human hip joints are shown in Fig. 8 and Fig. 9.

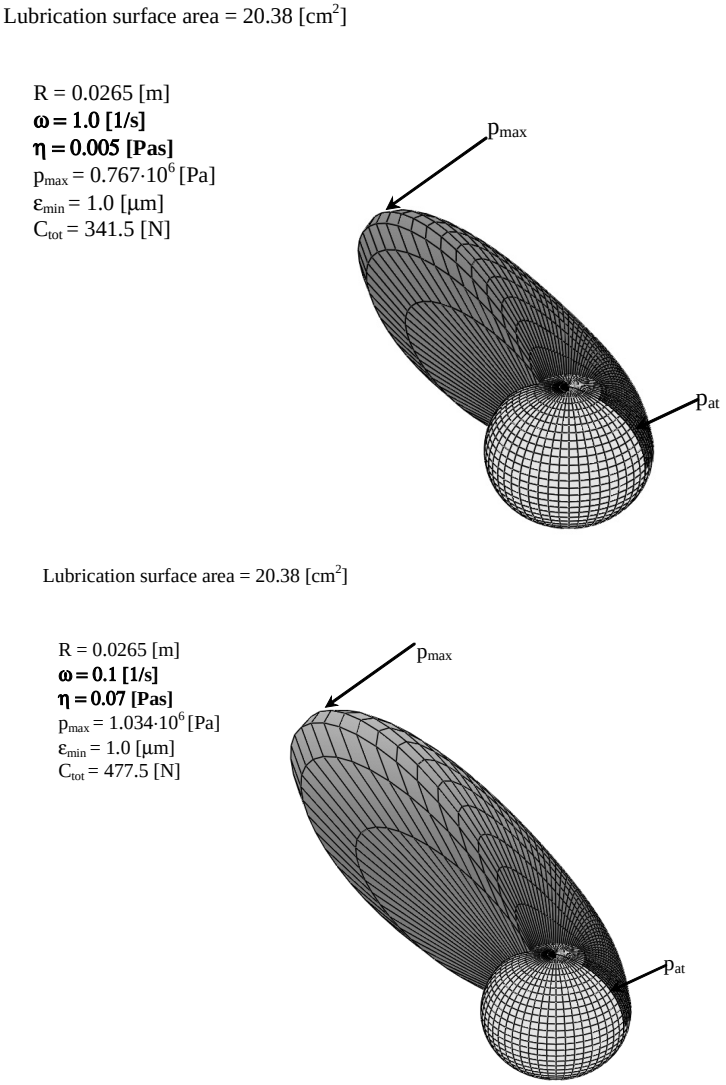

Fig. 9. Two cases of pressure distribution in pathological spherical hip joint gap during hydrodynamic lubrication caused by rotation
Fig. 9. Dwa przypadki rozkładu ciśnienia dla chorego sferycznego stawu biodrowego podczas hydrodynamicznego smarowania wywołanego ruchem obrotowym

For the capacities of 897 N, 673 N occurring in the normal joint, we obtain the following compressive stresses: $\tau_s = 897$ N/20.38 cm^2 = 0.43 N/mm^2 = = 0.43 MN/m^2 and $\tau_s = 673$ N/20.38 cm^2 = 0.33 N/mm^2 = 0.33 MN/m^2. In the pathological joint, the compressive stresses are as follows: $\tau_s = 341$ N/20.38 cm^2 = = 0.16 N/mm^2 = 0.16 MN/m^2 and $\tau_s = 477.5$ N/20.38 cm^2 = 0.23 N/mm^2 = = 0.23 MN/m^2. These stresses are smaller than the compressive strength of human joint cartilage ranging from 1.0 to 21 MN/m^2 [8], [9].

Numerical calculations were done by using Mathcad 12 Professional Program and the Method of Finite Differences. This method satisfies the requirement of the stability of numerical solutions of pressure function in the partial differential modified Reynolds Equations of the second order with variable coefficients in the form (8.1).

We impose atmospheric pressure on the curvilinear boundaries of the region $\Omega(\alpha_1,\alpha_3)$ located on the surface of the bone head in human hip joint.

Dynamic viscosity of synovial fluid decreases as shear rate increases. Shear rate of synovial fluid increases if the angular velocity ω, of head of human hip joint increases or joint gap height decreases. In the presented calculations, these changes are taken into account.

8.1. Conclusions

For the large shear rates, $100\ s^{-1} \le \Theta \le 1000\ s^{-1}$, the synovial fluid viscosity is as small as 10^{-1} Pas$\le\eta\le$1 Pas. In this case, we obtain the small pressure changes reaching from 2% to 4%. For small shear rates, $10^{-1}\ s^{-1} \le \Theta \le 10\ s^{-1}$, the viscosity is large, i.e. 10 Pas$\le\eta\le$100 Pas. In this case, by virtue of above calculations, we obtain pressure changes reaching from 7% to 15%.

Manuscript received by Editorial Board, September 09, 2007

References

[1] Biot M.A. General theory of three-dimensional consolidation, Journal of Applied Physics, 1941, Vol. 12, pp. 155–164.

[2] Garcia J.J., Altiero N.J., Haut R.C. Estimation of in situ elastic properties of biphasic cartilage based on a transversely isotropic hypoelastic model, Journal of Biomechanical Engineering, 2000, Vol. 122, pp. 1–18.

[3] Hlaváček M. Lubrication of the human ankle joint in walking with the synovial fluid filtrated by the cartilage with the surface zone worn out: steady pure sliding motion, Journal of Biomechanics, 1999, Vol. 32, pp. 1059–1069.

[4] Hsu F.H. The influences of mechanical loads on the form of a growing elastic body, Journal of Biomechanics, 1968, Vol. 1, pp. 303–313.

[5] Mow V.C., Kuei S.C., Lai W.M., Armstrong C.G. Biphasic creep and stress relaxation of articular cartilage in compression: theory and experiments, Journal of Biomechanical Engineering, 1980, Vol. 102, pp. 73–84.

[6] Скульский О.И., Аристов С.Н. Механика аномально вязких жидкостей, Москва–Ижевск: НИЦ «Регулярная и хаотическая динамика» (*in Russian*), 2004, pp. 156.
[7] Taber L. Nonlinear theory of elasticity. Application to biomechanics, World Scientific Publishing Co. Pte. Ltd., New Jersey, London, Singapore, 2004.
[8] Wierzcholski K. Bio- and Slide Bearings: Their Lubrication by Non-Newtonian Fluids and Application in Non-Conventional Systems. Volume I: Principles of Human Joint Lubrication with Non-Newtonian Liquids for Deformable Bone and Cartilage in Magnetic Field, Gdańsk University of Technology, Gdańsk, 2005.
[9] Wierzcholski K. Hip joint lubrication after injury for stochastic description with optimum standard deviation. Acta of Bioengineering and Biomechanics, 2005, Vol. 7, No. 2, pp. 13−40.

Acknowledgement

This research project has been supported by a Marie Curie Transfer of Knowledge Fellowship of the European Community´s Sixth Framework Program under contract number MTKD-CT-2004-517226.

Wkład do smarowania biołożysk

S t r e s z c z e n i e

Niniejsza praca przedstawia ogólny opis problemu smarowania dwóch żywych współpracujących ze sobą powierzchni chrząstki stawowej człowieka, oddzielonych płynem smarującym w warunkach niestacjonarnego przepływu. Płyn smarujący ma właściwości lepko-sprężyste. Uwzględniany jest wzrost oraz deformacja chrząstki stawowej. W przedstawionym problemie o charakterze bio-tribologicznym przyjęto genetyczny tensor wzrostu oraz deformacji współpracujących ciał traktowanych jako materiał łożyskowy.

Rozpatrywane warstwy wierzchnie chrząstki stawowej posiadają w mniejszym zakresie właściwości sprężyste, natomiast dominują właściwości podsprężyste oraz hypersprężyste.

Ten fakt ma wpływ na założone warunki brzegowe w szczelinie stawu człowieka. Jako szczególny przypadek omówiono materiał łożyskowy o właściwościach izotropowych.

Przykłady numeryczne rozkładów wartości ciśnienia hydrodynamicznego w zakresie tarcia płynnego oraz granicznego na powierzchni sferycznej głowy kostnej stawu biodrowego człowieka obejmują efekty wywołane ruchem obrotowym, jak również wyciskaniem płynu smarującego.